

Photodarkening, structural instabilities, and crystallization of glassy As_2Se_3 induced by laser irradiation

I. Abdulhalim,* R. Beserman, and R. Weil

Department of Physics and Solid State Institute, Technion-Israel Institute of Technology, Haifa 32000, Israel

(Received 28 March 1989; revised manuscript received 3 August 1989)

cw-laser-induced structural transformations in glassy As_2Se_3 have been studied as a function of the irradiation time using light scattering techniques. The behavior of the material under the influence of the laser irradiation is divided into five stages with respect to the irradiation level: (1) For low intensities ($I < 1.0 \text{ kW/cm}^2$), the Rayleigh and Raman scattering intensities show a decay with the irradiation time which is interpreted as due to photodarkening; (2) For irradiation levels ($1.0 < I \leq 1.7 \text{ kW/cm}^2$) the Raman peak position and width show quasiperiodic changes with the irradiation time; (3) At intermediate laser intensities ($1.7 < I \leq 1.95 \text{ kW/cm}^2$) below the threshold intensity for crystallization additional crystallinelike Raman peaks appear and disappear quasiperiodically; (4) For somewhat higher intensities ($1.95 \leq I \leq 2.1 \text{ kW/cm}^2$) close to the threshold for crystallization, the crystallinelike Raman peaks appear and disappear for some time but after that they increase and saturate; (5) For intensities above a threshold ($I > 2.1 \text{ kW/cm}^2$) the Rayleigh scattering and the crystalline Raman peaks grow rapidly and saturate after a short time to a height which depends on the intensity. We propose a model based on the existence of different metastable states in the glassy matrix having different degrees of disorder and on an athermal laser pumping mechanism of the irradiated material between these metastable states. We start from the photodarkening phenomenon at very low irradiation levels which correspond to transitions between only two states, and the enhancement of more atomic transitions at higher pumping rates up to the formation of submicrocrystalline clusters and their annealing or sequential internal transformations near the glassy-to-crystalline transition and finally their coalescence to form stable microcrystallites above some threshold intensity.

I. INTRODUCTION

Photoinduced structural modifications in chalcogenide glasses have been a subject of considerable interest both from fundamental and practical points of view. These light-induced effects could be divided mainly into three groups¹⁻³ with respect to the irradiation level: (1) at low irradiation levels up to the order of 100 mW/cm^2 , (2) at intermediate irradiation levels up to the threshold energy required for crystallization, and (3) above the threshold intensity where crystallization starts.

In the first region¹ there exists the photodarkening effect and other related changes in the physical properties of the chalcogenides such as the increase in the film thickness, the increase in index of refraction, and the increase in the optical absorption in the band-tail region.⁴ A decrease of the photoluminescence intensity⁵ and the infrared absorption⁶ (the appearance of an absorption band near midgap,⁷ an ESR signal,⁵ and induced optical anisotropy) are also seen.⁸ Most of these effects are reversible upon laser annealing and enhanced at photon energies lower than the energy gap and at low temperatures.

In the second energy region optical bistability and the oscillatory behavior of the transmittance and reflectance have been observed² in $g\text{-GeSe}_2$. These phenomena occur in a narrow intensity range and with photon energy less than that of the absorption edge. In the high irradiation level range, crystallization could be achieved either by

pulsed or by continuous-wave laser irradiation. Recently Balkanski *et al.*⁹ have studied chalcogenide glasses using photon energies higher than the band gap at $T \approx 300 \text{ K}$ as a function of the laser power and of the irradiation time. An important result of these studies is that the cw-laser-induced annealing process may be essentially athermal, as was suggested by Phillips.¹⁰

In a previous paper, we have reported¹¹ on a new instability effect in glassy As_2Se_3 . We found that crystalline Raman peaks appear and disappear quasiperiodically during the irradiation time in the intermediate irradiation levels range. In the present work we concentrate our attention on the changes in this range of very low irradiation levels. We observed a decay in the Raman scattering intensity and in the elastic scattering. Furthermore we present quasiperiodic changes in the Raman peak position and width against the irradiation time for intensities just below those required for the quasiperiodic behavior of the crystalline peaks. We analyze more extensively the oscillatory behavior and propose an athermal laser pumping mechanism. The nature of the metastable states in $g\text{-As}_2\text{Se}_3$ and the possible laser-induced transformations between them are considered. We start from the various molecular species which form the glassy state and the creation of molecular clusters which could be in different configurations until the small crystalline clusters are formed. These can then grow to form large microcrystallites at high irradiation levels after a sufficiently long irradiation.

II. EXPERIMENT AND RESULTS

The 0.5- μm -thick samples of glassy As_2Se_3 were prepared by standard evaporation on a quartz substrate.¹² The HH (incident and scattered polarizations parallel) polarized Stokes-Raman spectra between 150 and 500 cm^{-1} were measured as a function of the irradiation time using the backscattering geometry with the exciting 514.5-nm laser line at room temperature, in open air. The laser beam was focused on the sample surface to a spot of $\approx 140 \mu\text{m}$ diameter. The time required for scanning one spectrum is about 5 min. The measurements at different laser intensities were done on different positions on the sample in order to be sure that our starting point was always the glassy state. The spectral resolution of the Raman system is about 4 cm^{-1} achieved by a double monochromator.

Typical Stokes-Raman spectra in the range 150–450 cm^{-1} are shown in Fig. 1 in the case of very low irradiation levels ($I=0.98 \text{ kW/cm}^2$) for different irradiation

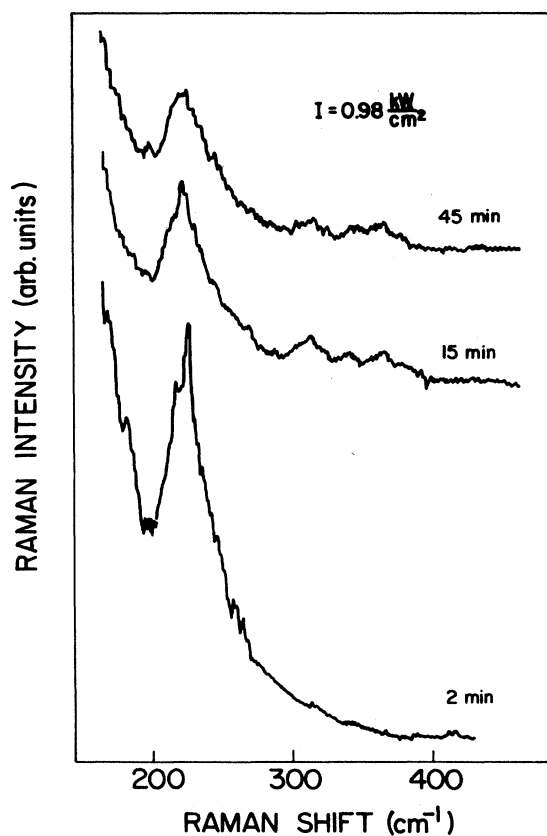


FIG. 1. The HH Raman spectrum of $g\text{-As}_2\text{Se}_3$ between 150 and 500 cm^{-1} at low irradiation level $I=0.98 \text{ kW/cm}^2$ at different irradiation times taken sequentially one after the other. The laser wavelength is $\lambda=514.5 \text{ nm}$. The irradiation times are measured from the beginning of irradiation until the peak maximum at 228 cm^{-1} is reached. The scale for the scattered intensity is the same, and the spectra were taken under the same experimental conditions.

times taken sequentially one after the other. The indicated irradiation times are measured from the beginning of the irradiation until the amorphous peak maximum at 228 cm^{-1} is reached. The spectrum of $g\text{-As}_2\text{Se}_3$ in the measured region consists mainly of the broad peak centered at around 228 cm^{-1} which corresponds to the antisymmetric As-Se-As stretching mode. The most prominent changes in the Raman spectra of Fig. 1 are the decay of the peak height with the irradiation time. The scattered intensity in the low-frequency side exhibits a parallel decay with irradiation time. There are no Raman peaks of $g\text{-As}_2\text{Se}_3$ in this frequency range. Therefore we attribute this scattered light to elastic Rayleigh scattering. We propose that the decay in the elastic Rayleigh and the inelastic Raman scattering intensities are due to the same process of photodarkening.¹ In Sec. III A we shall give a more complete explanation of this phenomenon. As the pumping level increases, the Raman peak starts to exhibit quasiperiodic changes in the peak position and width as shown in Fig. 2 when $I=1.59 \text{ kW/cm}^2$ and $\lambda=514.5 \text{ nm}$. Here one can observe a reduced decay in the elastic and inelastic scattering from the one observed when the pumping levels are lower.

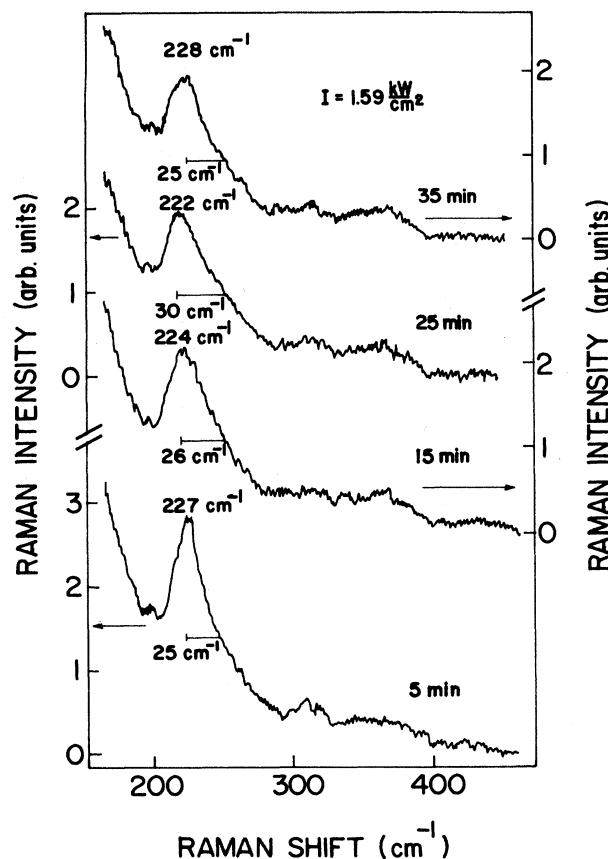


FIG. 2. Raman spectra of $g\text{-As}_2\text{Se}_3$ at $I=1.59 \text{ kW/cm}^2$ and $\lambda=514.5 \text{ nm}$ showing one cycle of the oscillatory changes.

This is due to the fact that as the laser intensity increases, the photodarkening process becomes faster and it becomes difficult to observe the decay in the scattered intensity from the beginning of the irradiation. The decay time is about 10 min, which is about the time interval between two consecutive Raman spectra. Consequently, in order to measure clearly this decay of the scattering intensities, one has to scan with higher speed and smaller frequency interval. This is the reason why we did not pay attention to this decay in our preliminary results.¹¹

The changes in the Raman peak position and width as a function of the irradiation time are plotted in Fig. 3. One observes inverse correlation between the peak position and width. As the peak shifts to higher frequency it becomes narrower, which indicates a more ordered state.

The decay of the scattered Raman intensity against the irradiation time is plotted in Figs. 4 and 5 for the glassy Raman peak and the elastic scattering at $\lambda = 518$ nm, respectively. There is no strong intensity dependence, except for the fact that at higher intensities, the decay is faster, and therefore it is difficult to follow the decay from the beginning of irradiation. However, when the intensity is in the second irradiation level range the amorphous Raman peak becomes structured and, when crystallization starts, it disappears. Simultaneously, the elastic scattering increases sharply, as shown in Fig. 5, for $I = 1.96$ kW/cm². At intermediate laser intensities the broad amorphous peak shape changes with the irradiation time. Figure 6 shows the temporal evolution of the Raman spectrum at $I = 1.85$ kW/cm². The most prominent feature is the appearance and the disappearance of the crystalline-like additional peaks superimposed on the amorphous band. We follow the evolution of the crystalline peak at 260 cm⁻¹, as a function of laser irradiation time. This peak is a normal mode of crystalline As₂Se₃. The quasiperiod t_2 of the oscillation increases with the irradiation time and the peak height tends to saturate after a long enough irradiation time. For higher irradiation levels close to, but still below, the threshold for crystallization (Fig. 7) the oscillatory behavior exists during some time interval t_3 which depends on the power level; after that time the crystalline peaks grow and saturate to intensities which depend on the irradiation level. During the first 30 min, the behavior is oscillatory; then the peak

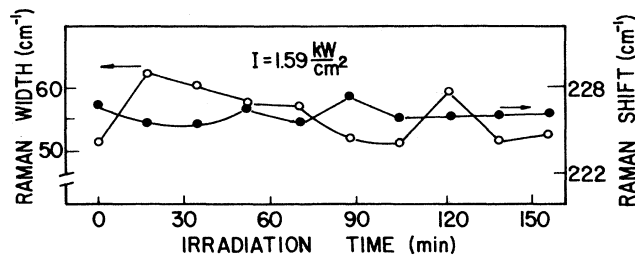


FIG. 3. Raman peak position (solid circles) and width (open circles), conditions of Fig. 2.

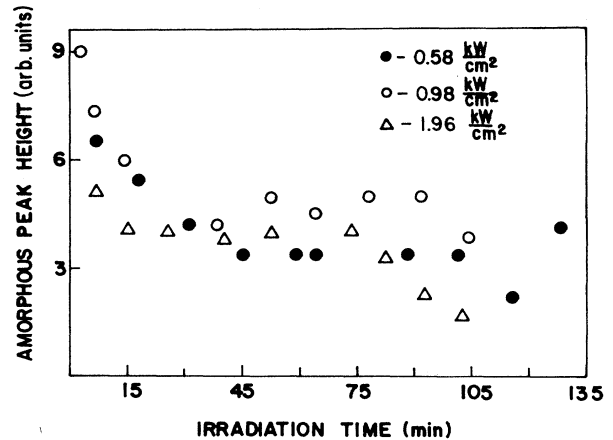


FIG. 4. Plot of the amorphous Raman peak height of 228 cm⁻¹ as a function of the irradiation time for different intensities showing the decay at low intensities due to photodarkening. At the relatively high intensity 1.96 kW/cm² (triangles) the peak becomes structured after 70 min and it starts to disappear due to crystallization. $\lambda = 514.5$ nm.

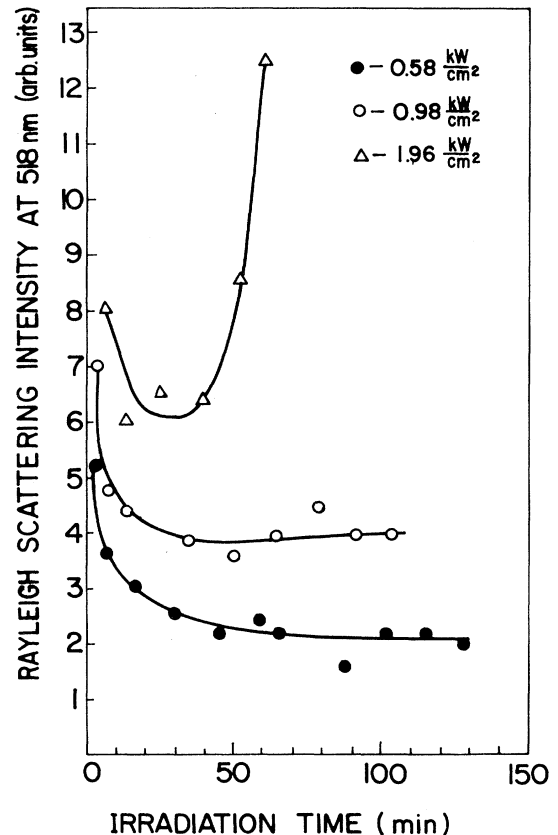


FIG. 5. The Rayleigh scattering intensity measured at 518.0 nm as a function of the irradiation time for the same intensities of Fig. 4. Laser $\lambda = 514.5$ nm.

at 260 cm^{-1} starts to rise rapidly and many other crystalline peaks start to appear. Up to this stage the Raman spectrum undergoes several changes as a function of the irradiation time. The amorphous band splits into two peaks first, then into three, and finally all of these peaks disappear, while only one crystalline peak at 190 cm^{-1} persists. The high-frequency side consists of many peaks at the beginning of illumination, which appear and disappear during the evolution process.

The laser intensity interval where the time t_3 is finite is very small. In our case, the range is between $1.95 \leq I < 2.1\text{ kW/cm}^2$. Above this intensity the crystalline peaks grow rapidly (Fig. 8) without oscillatory changes and reaches a saturation level which is the function of the incident laser intensity. The saturation time t_4 becomes very small as the intensity increases. The definition of the threshold intensity will be the intensity at which t_4 vanishes. In Fig. 9 we plot the crystalline peak intensity at 260 cm^{-1} normalized to the amorphous intensity background, as a function of irradiation time for different laser intensities showing the main properties of the evolution process as described in Figs. 6–8.

Whenever changes occur in the Raman spectrum as a function of the irradiation time, the system is reversible. That is—if the light is blocked off for a long enough

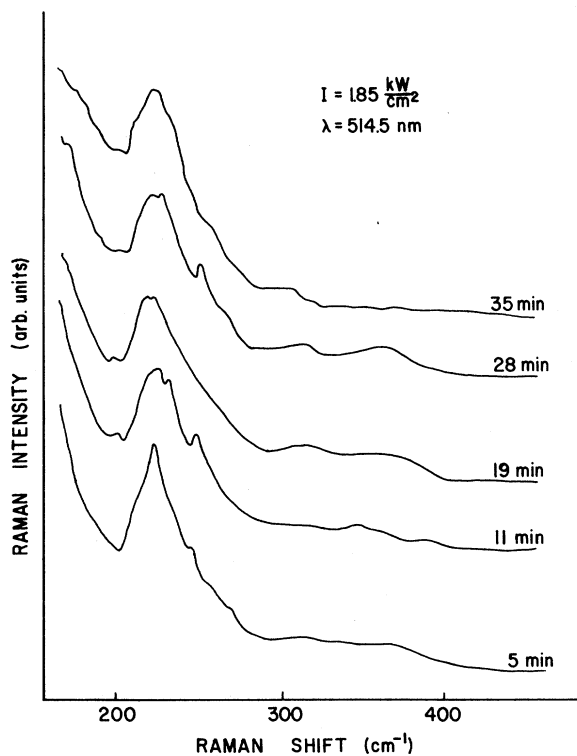


FIG. 6. Raman spectra at intermediate irradiation levels $I = 1.85\text{ kW/cm}^2$ for different irradiation times showing the appearance and disappearance of small crystalline peaks. $\lambda = 514.5\text{ nm}$.

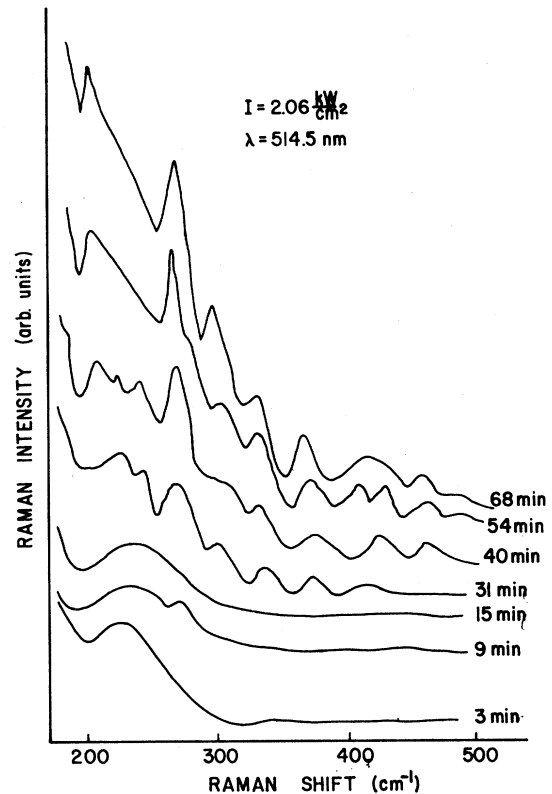


FIG. 7. Raman spectra at intensities just before the threshold for crystallization at different irradiation times. $I = 2.06\text{ kW/cm}^2$. $\lambda = 514.5\text{ nm}$.

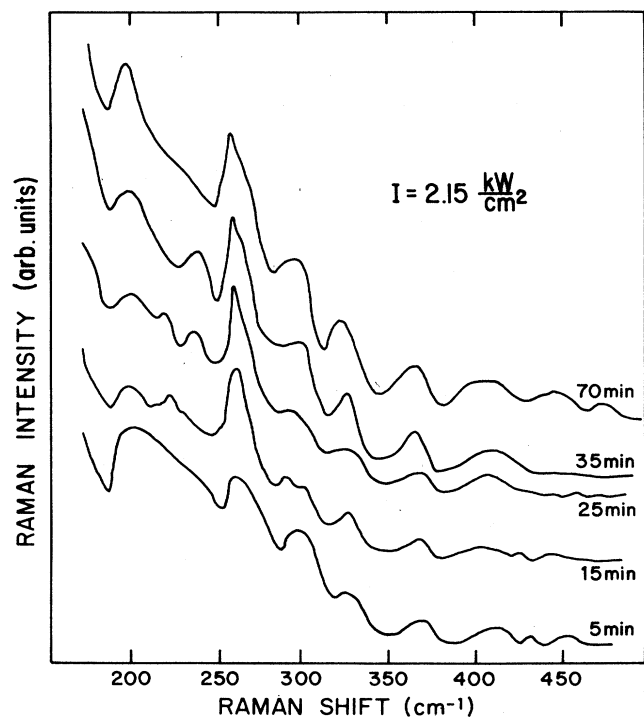


FIG. 8. Raman spectra at high irradiation levels. The crystalline peak grows gradually until a saturation is achieved after sufficient time of irradiation. $I = 2.15\text{ kW/cm}^2$, $\lambda = 514.5\text{ nm}$.

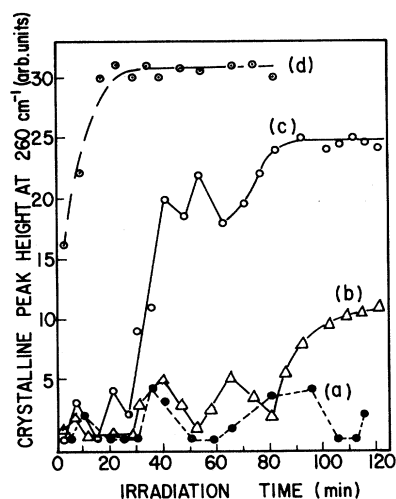


FIG. 9. The 260-cm^{-1} crystalline Raman peak intensity measured with respect to the amorphous background as a function of the irradiation time. The four stages of crystallization are shown: (a) 1.85 kW/cm^2 , (b) 1.96 kW/cm^2 , (c) 2.06 kW/cm^2 , and (d) 2.15 kW/cm^2 .

time, which depends on the amount of the radiation energy injected into the irradiated volume, the system will relax back to its initial state. However, if the changes in the Raman spectrum have reached saturation, the system will remain in its final state. The Stokes-Raman peaks, which persist in the final state, are at frequencies 190 , 260 , 292 , 327 , 363 , 414 , 450 , 475 , and 502 cm^{-1} . This is in agreement with the reported Raman spectra of crystalline As_2Se_3 by Zallen *et al.*¹³ in the frequency range up to 275 cm^{-1} . The differences between the two sets of results could be due to the fact that the final state is only a microcrystalline state, while in the work of Zallen *et al.*,¹³ the material was monocrystalline. Furthermore these microcrystallites are embedded in a glassy matrix and undergo large stresses from the surrounding. In addition, the effect of the laser is not only to cause annealing of the material; many other light-induced effects exist, as mentioned in the Introduction,¹⁻³ and a chalcogenide glass may polymerize partially because of photochemical reactions. Here we should note that Cernogora *et al.*¹⁴ have reported that the high-energy side of Raman spectra of $g\text{-As}_2\text{Se}_3$ grows near 260 cm^{-1} after illumination at very low temperatures (1.6 K). Their explanation is based essentially on changes in the local atomic configuration under the influence of the laser irradiation, which supports the athermal annealing process. The crystallization could be achieved either by irradiation for a long enough time with a power level close to the threshold or by increasing the power level above the threshold for a short time of irradiation. In Fig. 10 we show that the first spectrum taken with different irradiation levels on different virgin spots on the sample surface exhibits a transition from the glassy state to the crystalline state when the laser intensity is increased. The determination

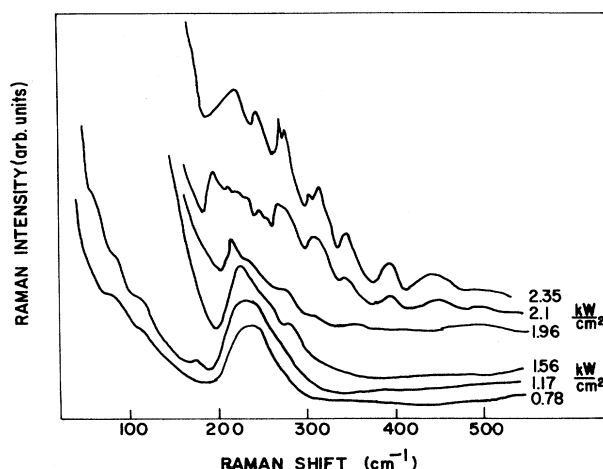


FIG. 10. The first Raman spectra measured with different intensities at different virgin spots on the sample surface. $\lambda = 514.5\text{ nm}$.

of the threshold intensity is achieved by plotting the crystalline peak height at 260 cm^{-1} against the laser intensity as in Fig. 11. It shows a sharp increase above a certain intensity and it saturates when the intensity is high enough. The threshold intensity is $\approx 2.2\text{ kW/cm}^2$ which is the value obtained if one plots the saturation time t_4 , as a function of intensity, and extrapolates to time zero. The elastic scattering also shows a similar behavior as a function of the irradiation intensity.

The high-energy Raman peaks have not been reported before in the literature. Some of them could be overtones of the Raman active low-frequency phonons. Some of these peaks have been measured by far-infrared absorption.¹⁵ Furthermore, there exists a controversy between different authors¹³⁻¹⁵ on the nature of the normal modes

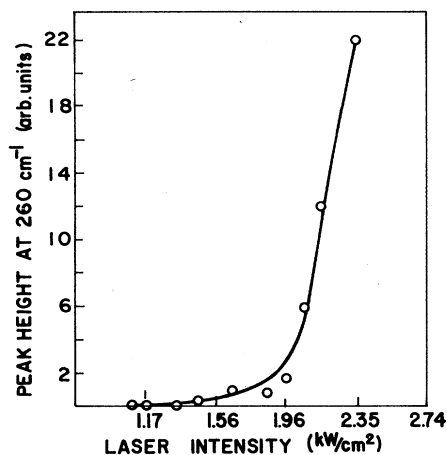


FIG. 11. The 260-cm^{-1} crystalline Raman peak intensity as a function of the laser intensity.

in crystalline As_2Se_3 . Its structure¹⁶ is layered with a slightly distorted orthorhombic unit cell containing four molecules, that is 20 atoms per unit cell each. Each atom is surrounded by three Se atoms which are nearest neighbors and form a slightly irregular pyramid. Each Se atom is bonded to two As atoms. The pyramids are linked by the corners to form a sheet structure, in which the atoms are arranged in 12-membered rings. The expected number of normal vibrations is 60 of which 30 are Raman active. We shall explain in what follows the decay in the Rayleigh and Raman scattering intensities at very low irradiation levels due to photodarkening. We propose the athermal pumping mechanism and explain the oscillatory behavior at intermediate irradiation levels, the instabilities near the glass-to-crystalline transition, and the kinetics of crystallization above a certain threshold intensity. Furthermore, we concentrate more on the nature of the metastable states in $g\text{-As}_2\text{Se}_3$ and the possible transformations between them induced by the laser irradiation.

III. DISCUSSION

Light scattering is a probe of the structural modifications in amorphous materials. As the amorphous Raman peak becomes narrower, the amorphous matrix is more ordered. For the TO-like peaks, this is usually accompanied with a shift toward higher frequencies. As the order increases, additional peaks may appear which correspond to new long-range order vibrations. In the case of amorphous As_2Se_3 , the main contribution to the Raman spectrum is due to the stretching vibrations associated with As-Se, because normal vibrations associated with long-range order are absent. Changes in the peak position and width are therefore a result of atomic transitions between different short-range-ordered states in the glassy matrix. As the laser intensity increases, intermediate range order is induced which manifests itself by the appearance of small ordered molecular clusters. For higher irradiation levels the cluster size increases and long-range order is built up. These laser-induced modifications are seen directly by the evolution of the Raman spectrum with the irradiation time at different intensities. We shall discuss these modifications in what follows starting from the glassy state where photodarkening takes place at very low irradiation levels up to the formation of a stable crystalline state above some threshold intensity.

A. Photodarkening probed by light scattering

1. Rayleigh scattering

Rayleigh scattering in glasses yields fundamental information about the state of a glass, namely, how the spatial fluctuations in macroscopic parameters deviate from those at thermodynamic equilibrium.¹⁷ The scattering intensity for small fluctuations in the Born approximation is proportional to the space-time Fourier transform of the correlation function $\langle \Delta\epsilon(\mathbf{r}+\mathbf{r}',t+t'), \Delta\epsilon(\mathbf{r},t) \rangle$ of the fluctuations in the dielectric constant $\Delta\epsilon(\mathbf{r},t)$. Rayleigh

scattering is a result of density fluctuations due to macroscopic inhomogeneities which do not exist in perfect crystals (see Fig. 12). The correlation length in this case is very large, but the fluctuation itself is very small. In disordered materials the lack of periodicity causes a shortening of the correlation range. That is, the correlation function $C(r')$ will decay spatially with some characteristic correlation length Λ . This decay is model dependent. Here we choose an exponential decay, as in the case of the Shuker-Gammon¹⁸ or Booker-Gordon¹⁹ models:

$$C(r') = C(0) \exp\left[-\frac{r'}{\Lambda}\right]. \quad (1)$$

In case of $K\Lambda \ll 1$, the cross section σ for scattering intensity is

$$\sigma \simeq \frac{16}{3} K^4 C(0) \Lambda^3 V, \quad (2)$$

where K is the wave number. Hence, the contribution to the scattering is proportional to the total scattering volume V and to the correlation volume Λ^3 .

The decay which is observed in the Rayleigh scattering in Figs. 1 and 5 is explained by Eq. (2). The increase in absorption due to photodarkening results in a decrease in the penetration depth and consequently in the scattering volume which is inversely proportional to α . Therefore, an increase of $\Delta\alpha = 1.5 \times 10^4 \text{ cm}^{-1}$ will cause a decay of about 40% in the scattered intensity. The observed decay in Figs. 1 and 5 could reach 60%. This additional difference is interpreted as a result of a decrease in the correlation length Λ due to photodarkening. As it is well established today, the photodarkening is accompanied by the creation of structural defects and by more disorder. Consequently a shorter correlation range is expected which results in more decay of the scattered Rayleigh intensity. A more quantitative comparison could be

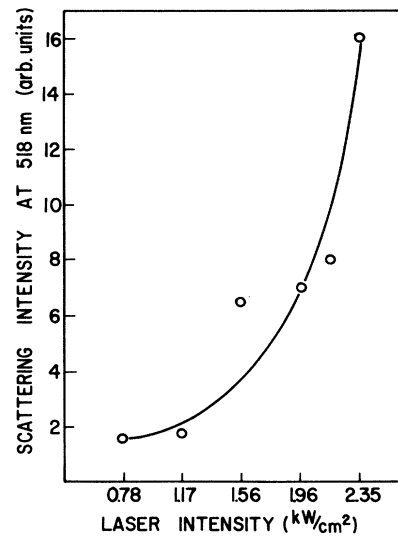


FIG. 12. Rayleigh intensity measurement at 518.0 nm as a function of the laser intensity. Laser $\lambda = 514.5 \text{ nm}$.

achieved by calculating the correlation length as a function of the parameters involved in the photodarkening process. Such a calculation may yield important information about the type and number of defects induced by irradiation due to the photodarkening process.

As the irradiation level increases, the material crystallizes above some threshold intensity and the Rayleigh scattering shows a sharp increase at that intensity as shown in Fig. 11. The difference in the absorption coefficients between the glassy and the crystalline state is very small at these photon energies and could not explain the sharp increase in Rayleigh scattering as the material crystallizes.

It may be possible that we observe a critical phenomena near the order-disorder phase transition. In order-disorder phase transitions the correlation length diverges near the transition to the ordered phase and is usually measured by light scattering. The determination of the critical exponent for Λ against the irradiation time and the irradiation level should yield fundamental information on the nature of the laser-induced order-disorder phase transitions in amorphous materials and the types of interactions which exist during the crystallization process.

2. Raman scattering

The first-order Raman scattering in amorphous materials was shown by Shuker and Gammon¹⁸ to be proportional to the phonon density of states $\rho(w)$, to the correlation volume Λ_σ^3 of a vibrational mode σ , and to the scattering volume V . The scattered intensity for an opaque material is given by the expression^{20,21}

$$I_{\{\alpha\}}^{(1)} = w_i^4 \left[1 - \frac{w}{w_i} \right]^3 \frac{S \delta |\tau_i \tau_s / \sqrt{\epsilon}|_{\{\alpha\}}^2}{2 \cos \theta_i} \times \sum_{\sigma} \frac{n(w_\sigma) + 1}{w_\sigma} \bar{C}_b^{\{\alpha\}}(w_\sigma) \rho_b(w_\sigma). \quad (3)$$

The summation is over all the modes σ in a vibrational band b . Here w_i and w_s are the incident and scattered photon frequencies, respectively. $w = w_i - w_s$ is the phonon frequency, r_i and r_s are the transmission coefficients for the incident and scattered radiation, respectively, n is the Bose occupation number, and ϵ is the complex dielectric constant. θ_i is the incidence angle. $\delta = \alpha^{-1}$ is the penetration depth. S is the illuminated area. $\{\alpha\}$ is the polarization configuration. The matrix element factor $\bar{C}_b^{\{\alpha\}}(w_\sigma)$, which represents the polarizability modulation by the modes σ in a band b , is referred to as the coupling parameter and is equal to $A_{\{\alpha\}} \Lambda_\sigma^3$ where $A_{\{\alpha\}}$ is a constant. The decay in the Raman peak height as observed in Figs. 1 and 4 due to photodarkening is straightforward according to Eq. (3). It is proportional to the transmission coefficients and to the increase of α . Let us assume that $\tau_i \approx \tau_s$. The decay in the transmission coefficient is about 70%, i.e., $\Delta\alpha \approx 1.5 \times 10^4 \text{ cm}^{-1}$, therefore the decay in the factor $|\tau_i \tau_s|^2 / \alpha$ in Eq. (3) is about 20%. On the other hand, the observed decay in the Raman-peak height is between 30–40%. This difference is attributed

to a decay in the correlation volume Λ_σ^3 which was expected, due to the increase in the degree of disorder, as in the case with the Rayleigh scattering. Again, a calculation of Λ_σ and its dependence on the degree of disorder could yield fundamental information on the light-induced photodarkening process.

B. Athermal laser pumping mechanism

At the irradiation levels used, we believe that the pumping mechanism is mainly athermal. (However, above a certain intensity the temperature of the irradiated volume rises rapidly and heating takes place.) The main fact upon which this assumption is based is that energy transfer from the hot mobile photoexcited electrons to the lattice is negligible at these levels. The thermalization time for the photoexcited electrons with the atoms is of the order of $\tau_T = \tau_e M / m_e \approx 10^{-10} - 10^{-9}$ sec and therefore the effective diffusion length is $l = (D_a \tau_T)^{1/2} \approx 10^{-3} - 10^{-4}$ cm which is apparently greater than the penetration depth $\delta \approx 10^{-5} - 10^{-4}$ cm (the diffusion constant, D_a , was calculated from the electronic drift mobility²² and Einstein's relation). This means that the photoexcited electrons created by the laser inside a layer of thickness $\delta < l$ can diffuse out of this layer without the emission of phonons. Furthermore the estimated photoexcited electron density in our case is $N_e \approx 10^{15} \text{ cm}^{-3}$, if one takes a relaxation time $\tau_e \approx 10^{-12}$ sec, the plasma frequency is thus about $\omega_p \approx 30 \text{ cm}^{-1}$. This is much less than the photoelectrons energy $\hbar\omega_i - Eg \approx 0.7 \text{ eV}$ and consequently the rate of plasmon emission is very small. In addition, this plasma frequency ω_p is much smaller than the phonon frequency and therefore the rate of phonons emission due to plasmon-phonon coupling is negligible.²³ In other words, the energy is stored in the photoexcited electrons system during a time $\tau_T \approx 10^{-10} - 10^{-9}$ sec and no energy transfer to the lattice in the form of heat takes place during this time. After this time the electrons diffuse out of the interaction volume. We independently measure the temperature from the ratio of Stokes to anti-Stokes; it does not vary during the experiment. Our experimental results concerning the temperature estimation from the Stokes to anti-Stokes ratio, the existence of the oscillatory behavior, the reversibility effect, and the properties of kinetics of crystallization support the nonthermal pumping process as will be further explained.

The question which arises thus is what mechanisms cause the material in the interaction region to rearrange in different structural configurations under the influence of laser irradiation. Recently, we proposed a microscopic mechanism.²⁴ It is based on the existence of short-lived large-energy fluctuations of atoms inside the solid.²⁵ When these fluctuating atoms jump from one metastable state to another, they stretch and cutoff bonds with neighbors. This leads to the formation of transient local electronic levels of lifetime $\Delta\tau_e$ of the same order of magnitude as the fluctuation lifetime $\Delta\tau \approx 10^{-13} - 10^{-12}$ sec. Then the photoelectrons created could be trapped in these local electronic levels and release their energy in the vicinity of the hopping particles, increasing the probabili-

ty of the transition between the two metastable states over the energy barrier. These transitions of the atoms assisted by the interaction with the hot mobile electrons change the material structure and cause the changes in the Raman width and position of the absorption edge and other related parameters. This is the sense of athermal pumping. The material is pumped athermally from one metastable state to another more ordered one with a pumping rate which depends on the incident photon flux and other characteristic parameters of the material (electronic effective mass and charge, relaxation times, quantum efficiency, etc.) The pumping rate determines both the final saturation state, achieved after sufficient irradiation time, and the way the system evolves to reach this state.

The estimated characteristic time of the atomic transitions was shown²⁶ to play a crucial role in the determination of the quasiperiod of oscillations, in the case of irradiation levels lower than the threshold. When crystallization occurs, however, the calculation does not hold, because crystallization is a cooperative phenomenon, where the interaction between clusters of different sizes takes place under the influence of laser pumping. Furthermore for high irradiation levels above the threshold some heating exists and one must be able to distinguish between thermal and athermal pumping mechanisms for the analysis of the laser-induced crystallization phenomena.

C. Structural instabilities and crystallization

1. Mechanism for oscillations at low irradiation levels

The pumping mechanism proposed in the last section suggests the existence of different metastable states in the glassy matrix. In the region of low irradiation levels up to 1.9 kW/cm², where the material is still glassy, the metastable states have several structural configurations with different degrees of disorder. Under the influence of laser irradiation the material is pumped between these metastable states resulting in the observed oscillations. A calculation for the prediction of the quasiperiod has been given in our previous paper.²⁴

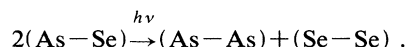
2. Metastable states in *g*-As₂Se₃ and the laser-induced modifications at low irradiation levels

The chalcogenide glasses are believed to be formed into a fully cross-linked random network connecting the atomic units. The nature of these atomic units is not well known, but in the literature various structures are proposed.²⁷⁻³³ Since Raman spectroscopy is sensitive to the local atomic units in the sample, the Raman oscillatory changes at low irradiation levels (Fig. 2) could be related to transformations between these molecular species under the influence of laser irradiation via photochemical reactions.

Hence the exact nature of the small molecular clusters forming the glass is not known, but at least all the models propose the existence of molecular species. This fact led us to propose a statistical model where different molecular species coexist. Under laser irradiation photochemical reactions may occur and increase the concentrations

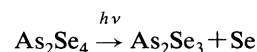
of the laser-induced clusters. One may consider the amorphous Raman peak at 228 cm⁻¹ to be the result^{13,34} of a broadening of the crystalline Raman peaks at 202, 215, 230, 247, and 272 cm⁻¹. These peaks are known to be molecular in their nature and fall in the region of the vibrational stretching modes of As—Se bonds which is between 150 and 300 cm⁻¹. Therefore changes in the concentration of one type of As—Se bonds due to photoreactions could result in changes in the peak position and width.

The primary effect of the light is to break bonds; additional atomic configurations may be formed if the laser pumping rate is high enough. As one possibility consider the following reaction:³⁵



After this reaction, the bond statistics of As₂Se₃ is shifted from a state which is close to the chemically ordered model toward a state described by the random network model. The randomness of the chemical bond distribution is therefore increased.

As the formation of As and Se clusters involves the absorption of several photons, the density of As—As and Se—Se bonds at a given temperature and wavelength depend on the irradiation level. Up to the irradiation levels where only the photodarkening occurs, the density of the created As—As and Se—Se bonds is only adequate to change the Rayleigh and Raman intensities. It is not adequate to change the Raman peak position and width. On the other hand, if the irradiation level is higher, the density of the As—As and Se—Se bonds becomes so high that they contribute to a weak Raman scattering near 250 cm⁻¹ following Nemanich *et al.*³⁶ This causes a shift and a broadening of the amorphous Raman peak at 228 cm⁻¹. However, this chemical reaction is thermodynamically unfavorable ($\Delta_G > 0$). The As and Se clusters formed by illumination can be dissolved and converted back to As—Se bonds. This could occur spontaneously due to their instability and their large concentration, which increases the restoring strain from the surrounding non irradiated material. This explains why in the photodarkening regime they could not be returned to As—Se bonds without heating. The above back and forth transformation could not explain the saturation behavior of the oscillations after a very long time of irradiation. For this purpose we introduce the fact that the homopolar bonds As—As or Se—Se may allow the existence of units, such as Se₂As—AsSe₂, which may undergo the light-induced reaction:



leading to the rearrangement of interatomic bonds and the creation of the stable units As₂Se₃ and a saturation is achieved when a large portion of the less stable units is transformed into the more ordered units such as As₂Se₃.

The explanation of the reversibility effect is now straightforward. Since the created As and Se clusters are unstable these clusters could be transformed back into As—Se bonds under the influence of the strain applied by

the surrounding nonirradiated material. When the light is blocked before a saturation state is achieved, the system will relax back to its original nonilluminated state.

The above-proposed transformation is not the only one which could occur under laser irradiation. Many other processes could happen depending on the initial molecular species which exist in a glassy matrix and how they react under photon absorption. The intermediate As and Se clusters themselves could form different configurations before the final stable atomic unit As_2Se_3 is maintained. The simplest clusters are those with two atoms As_2 and Se_2 which could dissolve back much more easily than clusters As_n with $n > 2$. Different configurations of the As_n and Se_n together must be formed before they transform into the stable unit As_2Se_3 such as the configuration As_2Se_4 in the above reaction. The existence of more than two such metastable states is a primary condition for the quasiperiodic behavior to occur.

3. Instabilities of small submicrocrystalline clusters at intermediate irradiation levels

By increasing the irradiation level $I > 1.9 \text{ kW/cm}^2$ the material is pumped faster toward a final stable glassy state where a large fraction of the different molecular species converted to As_2Se_3 units or to pyramidal units AsSe_3 . The breaking of these units requires higher energy, since they are stable enough and by appropriate orientation they form the layered structure of crystalline As_2Se_3 . It is more favorable now to create small clusters of these units. Such clusters themselves could then be in different configurations when their size is very small. One expects that above some critical size the clusters tend to have a more crystalline topology. This will allow the appearance of small crystalline Raman peaks as in Fig. 8. However, these submicrocrystalline clusters could be transformed between different configurations and dissolve to form smaller clusters of the atomic units As_2Se_3 under the influence of the strain³⁷ produced in the cluster-glass interface and explain the appearance and disappearance of crystalline Raman peaks.

After long exposure to light, a large fraction of the material in the interaction volume is converted and increases the submicrocrystalline clusters size causing the quasiperiod to increase and a saturation is achieved after very long time of irradiation, since the pumping rate is below the one needed to increase the cluster size above the value it reached. The average critical cluster size where stabilization is maintained is unknown for the case of $g\text{-As}_2\text{Se}_3$. In $\alpha\text{-Si}$ this critical size is about 30 Å; under this value the clusters in the diamond structure become unstable with respect to the amorphous state.¹⁵ In the present case we expect it to be larger, since one unit cell of crystalline As_2Se_3 contains 20 atoms. If the critical cluster is supposed to be a few unit cells in order to contribute to the crystalline Raman peaks, then one may expect a size of more than 60 Å.

4. Oscillations near the glass-to-crystal transition and the kinetics of crystallization

When the irradiation level is higher than in the previous intermediate region, the higher pumping rate allows

for the creation of larger concentrations of clusters with crystalline order in a short time which depends on the laser intensity. After this time interval no more oscillations occur and the clusters grow gradually. Some of them may grow by addition of newly oriented molecules to their surfaces, others—the smaller ones—will aggregate together and form larger clusters with an average size which increases rapidly. This latter phenomenon is enhanced now, since molecules can rotate more freely due to the free volume created by the difference in density between the glass and the submicrocrystalline clusters.

The oscillations stop, because the average size and concentration of the submicrocrystalline clusters reach values higher than those required for the reverse transformations to occur.

After some time interval t_4 the peak height and width saturate to values which depend on the irradiation level. The threshold intensity is the one at which the time required for saturation extrapolates to zero. The increase of the crystalline peak height and its narrowing indicate both an increase of the cluster's size and concentration. The small clusters can coalesce to form larger ones attaining a microcrystalline size after sufficient irradiation.

IV. CONCLUSIONS

The photodarkening process, structural instabilities at nucleation, and growth up to crystallization of $g\text{-As}_2\text{Se}_3$ driven by midrange cw laser irradiation were studied by light scattering. The temporal evolution of the system was found to show five different stages with respect to the irradiation level.

(1) At very low irradiation levels up to 1 kW/cm^2 the Rayleigh and Raman scattering intensities decay with irradiation time. This is explained by the photodarkening process through the dependence of the expressions for the Rayleigh and Raman scattering cross sections. We found that the observed decay is higher than the calculated one. This difference is attributed to the unknown decrease of the correlation length after the photodarkening process.

(2) For higher irradiation levels in the range $1.0 < I \leq 1.7 \text{ kW/cm}^2$ the Raman spectrum is still that of a glassy matrix, but it exhibits quasiperiodic oscillatory changes in the peak position and width function of the irradiation time. In this stage, the explanation is based on structural transformations of the glassy material inside the interaction region between different glassy metastable states having different degrees of disorder. These transformations are driven by the laser irradiation via non-thermal pumping mechanism. The effect of the surrounding nonirradiated material enters as a restoring strain, which promotes the backward transformations. Its action explains the reversibility effect, which exists when the system did not reach saturation. The different molecular species which could exist in a glassy matrix are considered as a basis for the metastable states where the transition between them occurs until more stable molecular units such as As_2Se_3 or AsSe_3 are formed which are the basic units for building the crystalline state.

(3) At intermediate irradiation levels $1.7 < I \leq 1.95$

kW/cm^2 the Raman spectrum shows additional small crystalline Raman peaks superimposed to the glassy peak which appear and disappear quasiperiodically with the irradiation time. In this stage the pumping rate is sufficiently high to excite the stable molecular units As_2Se_3 to form small clusters having a crystalline topology in their interior where their size have to be larger than 60 \AA for the associated crystalline Raman peaks to appear. However, such clusters could dissociate spontaneously or under the action of a slight laser heating, and the restoring strain from the glassy surrounding. The smaller clusters cannot contribute to the crystalline Raman peaks. This explains the reversibility effect in this regime.

(4) For intensities just below the threshold for crystallization $1.95 < I \leq 2.1 \text{ kW/cm}^2$ the crystallinelike Raman peaks appear and disappear for some time, but after a given threshold intensity is reached, saturation occurs. In this stage the pumping rate is sufficient to form clusters of bigger size and concentration such that after some time a large fraction of the material is transformed into the submicrocrystalline clusters. By further input of the radiation energy the cluster's size and concentration can increase and saturate when the pumping rate is compensated by the strain accumulated in the crystallites-glass interface.

(5) Above the previous region $I > 2.1 \text{ kW/cm}^2$ no more

oscillations occur. The crystalline Raman peaks grow gradually and saturate to a value which depends on the laser intensity. Above a certain intensity $I \approx 2.2 \text{ kW/cm}^2$ they increase sharply exhibiting a threshold behavior. The Rayleigh scattering intensity exhibits similar behavior. Here we propose that this threshold behavior is due to a some divergence of the correlation length near the disorder-to-order phase transition. Further investigation of this point could yield much information on the nature of glass-crystal transition.

The phenomena described in this paper exist in several disordered materials.³⁸ In our opinion, they are of importance toward the full understanding of the microstructure of glassy materials and the effect of irradiation on the glassy matrix. Correlation of these results with other types of measurements is required such as electron diffraction, ESR, photoluminescence, and photoconductivity for complete characterization of the metastable states in a glassy matrix. It would also be of interest to follow the evolution of the system under laser irradiation at different temperatures for the discrimination between thermal and athermal laser pumping mechanisms.

ACKNOWLEDGMENTS

We gratefully acknowledge the help of K. Weiser who provided the samples on which the measurements were made.

*Present address: University of Colorado, Department of Electrical and Computer Engineering—Center for Optoelectronic Computing Systems, Boulder, CO 80309-0425.

¹J. P. DeNeufville, in *Optical Properties of Solids—New Developments*, edited by B. O. Seraphin (North-Holland, Amsterdam, 1975), p. 137; see also a review paper by K. Tanaka, *J. Non-Cryst. Solids* **35&36**, 1023 (1980).

²J. Hajto, G. Zentai, and I. Kosa Somogyi, *Solid State Commun.* **23**, 401 (1977); J. Hajto, J. Janossy, and W. K. Choi, *J. Non-Cryst. Solids* **77&72**, 1273 (1985); J. Hajto and J. Janassy, *Philos. Mag. B* **47**, 347 (1983).

³*Laser and Electron-Beam Interactions with Solids*, Vol. 4 of the *Proceedings of the Materials Research Society, Boston, 1981*, edited by D. Appleton and G. K. Celler (MRS, Pittsburgh, 1980); *Laser-Solid Interactions and Transient Thermal Processing of Materials*, Vol. 13, *Proceedings of Materials Research Society, Boston, 1982*, edited by J. Narayan, W. L. Brown, and R. A. Lemons (MRS, Pittsburgh, 1981); *Interactions Laser-Solids* [*J. Phys. (Paris) Colloq.* **44**, C5-10 (1983)]; J. F. Gibbons, *Semiconductors and Semimetals* (Academic, New York, 1984), Vol. 17.

⁴J. Cernogora, F. Mollot, and C. Benoit à la Guillaume (unpublished).

⁵J. Cernogora, F. Mollot, and C. Benoit à la Guillaume, *Phys. Status Solidi A* **15**, 401 (1973); R. A. Street, T. M. Searle, and I. G. Austen, *J. Phys. C* **6**, 1830 (1973).

⁶F. Mollot, G. Cernogora, C. Benoit à la Guillaume, A. Ribeyron, and J. M. Laurant (unpublished).

⁷S. G. Bishop, U. Strom, and P. C. Taylor, *Phys. Rev. Lett.* **34**, 1346 (1975).

⁸V. G. Zhdanov, B. T. Kolomiets, V. M. Lyubin, and V. K. Malinovskii, *Phys. Status Solidi A* **52**, 621 (1979).

⁹M. Balkanski, E. Harom, G. P. Espinosa, and J. C. Phillips,

Solid State Commun. **51**, 639 (1984).

¹⁰J. C. Phillips, *Commun. Solid State Phys.* **10**, 165 (1982).

¹¹I. Abdulhalim and R. Beserman, *Solid State Commun.* **64**, 951 (1987).

¹²E. Zeldov and K. Weiser, *J. Non-Cryst. Solids* **59-60**, 965 (1983).

¹³R. Zallen, M. L. Slade, and A. T. Ward, *Phys. Rev. B* **3**, 12, 4257 (1971).

¹⁴J. Cernogora, F. Mollot, and C. Benoit à la Guillaume, *Solid State Commun.* **19**, 465 (1976); M. Onomichi, T. Arai, and K. Kudo, *J. Non-Cryst. Solids* **6**, 362 (1971); L. B. Zlatkin and Yu. F. Markov, *Phys. Status Solidi A* **4**, 391 (1971).

¹⁵I. G. Austin and E. S. Garbett, *Philos. Mag.* **23**, 17 (1971).

¹⁶K. Weiser, in *Amorphous Chalcogenides*, Vol. II of *Noncrystalline Semiconductors*, edited by M. Pollak (Chemical Rubber Co., Boca Raton, FL, 1987), p. 97.

¹⁷J. Tauch, in the *3rd International Conference on Light Scattering in Solids*, edited by M. Balkanski, R. C. C. Leite, and S. P. S. Porto (Flammarion, Paris, 1976), p. 621.

¹⁸R. Shuker and R. Gammon, *Phys. Rev. Lett.* **25**, 222 (1970).

¹⁹K. Ishimaru, *Wave Propagation and Scattering in Random Media* (Academic, New York, 1978), Vol. 2, Chap. 16.

²⁰M. V. Klein, J. A. Holy, and W. S. Williams, *Phys. Rev. B* **17**, 1546 (1978).

²¹J. S. Lannin, in *Raman Scattering of Amorphous Si, Ge and Their Alloys*, Vol. 21 of *Semiconductors and Semimetals*, edited by J. I. Pankove (Academic, New York, 1984), Chap. 6, Pt. B, pp. 159–195.

²²J. Orenstein, M. A. Kastener, and V. Vavilov, *Philos. Mag. B* **46**, 23 (1982).

²³E. J. Yoffa, *Phys. Rev. B* **21**, 2415 (1980).

²⁴I. Abdulhalim, Beserman, and Yu. L., Khait, *J. Non-Cryst. Solids* **97-98**, 387 (1987); *Europhys. Lett.* **4**, 1371 (1987); I.

- Beserman, I. Abdulhalim, Yu. L. Khait, and R. Weil, *Appl. Phys. Lett.* **51**, 1898 (1987); R. Beserman, I. Abdulhalim, and R. Weil, *Phys. Rev. B* **39**, 1081 (1989).
- ²⁵Yu. L. Khait, *Phys. Rep.* **99**, 237 (1983); Yu. L. Khait and R. Beserman, *Phys. Rev. B* **33**, 2983 (1986).
- ²⁶P. Bellon and G. Martin, *Phys. Rev. B* **38**, 2570 (1988).
- ²⁷G. Lucovsky and R. M. Martin, *J. Non-Cryst. Solids* **8-10**, 185 (1972); G. Lucovsky, *Phys. Rev. B* **6**, 4, 1480 (1972).
- ²⁸J. P. DeNeufville, S. C. Moss, and S. R. Ovschinsky, *J. Non-Cryst. Solids* **13**, 191 (1973).
- ²⁹D. J. Treacy, P. C. Taylor, and P. B. Klein, *Solid State Commun.* **32**, 423 (1979) and P. C. Taylor, S. G. Bishop, and D. L. Mitchell, *ibid.* **8**, 1783 (1970).
- ³⁰R. J. Nemanich, *Phys. Rev. B* **16**, 1655 (1977).
- ³¹A. J. Apling, A. J. Leadbetter, and A. C. Wright, *J. Non-Cryst. Solids* **23**, 369 (1977).
- ³²V. M. Bermudes, *J. Chem. Phys.* **57**, 7 (1972); **57**, 2793 (1972).
- ³³D. Babić and S. Rabić, *Phys. Rev. B* **38**, 10490 (1988).
- ³⁴E. Finkman, A. P. DeFonzo, and J. Tauc, in *Proceedings of the 12th International Conference on the Physics of Semiconductors*, edited by M. H. Pilkućin (Teubner, Stuttgart, 1974), p. 1022.
- ³⁵M. Frumar, A. P. Firth, and A. E. Owen, *Philos. Mag. B* **50**, 4 (1984); **50**, 463 (1984).
- ³⁶R. J. Nemanich, G. A. N. Conell, T. M. Hayes, and R. A. Street, *Phys. Rev. B* **18**, 6900 (1978); R. J. Nemanich, S. A. Solin, and R. M. Martin, *ibid.* **23**, 635 (1981).
- ³⁷J. Jortner, D. Scharf, and U. Landman, in *Energetics and Dynamics of Clusters, Excited State Spectroscopy in Solids*, Proceedings of the International School of Physics "Enrico Fermi," Varenna, 1986 (North-Holland, Amsterdam, 1987), p. 438.
- ³⁸I. Abdulhalim, Ph.D. thesis, Technion, Haifa, Israel, 1988.